Ultrahigh-Q Fano Resonances in Terahertz Metasurfaces: Strong Influence of Metallic Conductivity at Extremely Low Asymmetry

Srivastava, Yogesh Kumar; Al-Naib, Ibraheem; Zhang, Weili; Singh, Ranjan; Manjappa, Manukumara; Cong, Longqing; Cao, Wei

2016

Srivastava, Y. K., Manjappa, M., Cong, L., Cao, W., Al-Naib, I., Zhang, W., et al. (2016). Ultrahigh-Q Fano Resonances in Terahertz Metasurfaces: Strong Influence of Metallic Conductivity at Extremely Low Asymmetry. Advanced Optical Materials, 4(3), 457-463.

https://hdl.handle.net/10356/83779

https://doi.org/10.1002/adom.201500504

Article type: Full Paper

Ultrahigh-*Q* Fano Resonances in Terahertz Metasurfaces: Strong Influence of Metallic Conductivity at Extremely Low Asymmetry

*Yogesh Kumar Srivastava, Manukumara Manjappa, Longqing Cong, Wei Cao, Ibraheem Al-Naib, Weili Zhang, and Ranjan Singh**

Yogesh Kumar Srivastava, Manukumara Manjappa, Longqing Cong, Prof. Ranjan Singh
Division of Physics and Applied Physics, School of Physical and Mathematical Sciences, Nanyang Technological University, Singapore 637371, Singapore
Centre for Disruptive Photonic Technologies, School of Physical and Mathematical Sciences, Nanyang Technological University, Singapore 637371, Singapore
E-mail: ranjans@ntu.edu.sg

Wei Cao
School of Electrical and Computer Engineering, Oklahoma State University, Stillwater, OK 74078

Ibraheem Al-Naib
Biomedical Engineering Department, College of Engineering, University of Dammam, Dammam, Saudi Arabia

Prof. Weili Zhang
School of Electrical and Computer Engineering, Oklahoma State University, Stillwater, OK 74078

Key words:

Metamaterials, Fano resonance phenomena, conductivity, terahertz, high-*Q* resonance

Abstract

Fano resonances in metasurfaces are important due to their low loss subradiant behaviour that allows excitation of high quality (*Q*) factor resonances extending from the microwave to the optical regime. High *Q* factor Fano resonances have recently enabled applications in the areas of sensing, modulation, filtering and efficient cavities for lasing spasers. High conductivity metals are the most commonly used materials for fabricating the metasurfaces, especially at the low frequency terahertz region where the dc, Drude, and perfect electric conductivity provided similar resonant behavior of the meta-atoms. Here, we experimentally and theoretically demontrate that the *Q* factor of a low asymmetry Fano resonance is extremely

sensitive to the conducting properties of the metal at terahertz frequencies. To our surprise, we observe significantly different Q factor and figure of merit of the Fano resonance for perfect electric conductors, Drude metal and a dc conducting metal. Identification of such a low asymmetry regime in Fano metasurface resonators is the key to engineer the radiative and non-radiative losses in plasmonic and metamaterial based active and passive devices that have potential applications in the terahertz, infrared and the optical range frequencies.

Introduction:

Metamaterials are specially designed new class of artificially structured materials. Unlike natural materials, the optical behaviour of the metamaterials depends on their size, shape and structural arrangement of designer unit cell known as meta-atom and its resonant/non resonant response is due to their interaction in the lattice array instead of its chemical constituents.[1-5] Coupling of electromagnetic (EM) radiation in such periodic arrays can have enormous impact on light matter interactions.[6] These couplings result in high concentration of electric field and/or magnetic field in the planar metamaterials and can also be engineered to support sharp resonances with higher quality (Q) factors and intense field confinement within a small volume. High Q devices are mainly desirable for sensor applications[7-10] and non-linear processes.[11, 12] Most of the metamaterials are made up of metallic resonators that can support well defined resonances due to high conductivity. However, significantly high losses in metals have limited the possibility of efficient devices in optical, infrared and terahertz frequency ranges.

There are mainly two kinds of losses in the metamaterials that affect the linewidth of resonances namely, Ohmic (non-radiative) losses due to resistance of metals and radiative losses due to the subwavelength nature of the meta-atoms. Thus, the response of metamaterial is highly dependent on the losses present in constituent materials. Metals at terahertz frequencies are treated as near perfect electric conductors (PEC). However, we show in this contribution that the assumption of PEC becomes highly inaccurate for the case of high Q asymmetric Fano resonant metamaterial structures, where we found that the resonance behavior is extremely sensitive to the conducting properties of the resonators. High conductivity at terahertz frequencies enables low non-radiative losses but the Q factors are still limited by the radiative losses.[13-15]

There are three different hypothesis for the dispersion behaviour in metals, which are widely used in metamaterials especially in terahertz frequency band: PEC, Drude model for conductivity and dc conductivity of metal. As per the first hypothesis, metals as constituent material of metamaterials behave as PEC at terahertz frequencies due to their extremely high conductivity.[16] While according to the second assumption, the dispersion in metals is considered to follow the Drude theory of metals, which describes the frequency dependent dielectric constant and conductivity.[17] However, skin-depth scale metallic films at terahertz frequency behave differently from bulk metals because of additional electron scattering mechanism from grain boundaries and defects. In the third hypothesis, the dc conductivity of metals at terahertz frequency has also been used to explain the behaviour of metamaterial subwavelength resonators.[14] Conductivity of the metal according to Drude theory is given by _____, which reduces to in the lower frequency limits i.e. $\omega/\Gamma \ll 1$. In most of the previous terahertz metamaterial works, it is typical to either use the assumption of PEC or the dc conductivity of metallic subwavelength resonators. Both of these assumptions give similar results that agree reasonably well with the measurements.[14] However, in this contribution we discovered that the terahertz asymmetric Fano resonator[18-24] metamaterials show significantly different behaviour in terms of the resonance linewidths and the amplitude for all the three different types of material conductivity. The effect is more prominent in the sharp resonance regime that occurs at lower structural asymmetry in the Fano resonator where the radiative loss is low. For larger degree of asymmetry, the Fano resonance broadens due to higher radiative loss and in this regime, the response of the terahertz asymmetric split-ring resonators (TASRs) for the three different conductivity models is similar. Our measurements reveal that the experimental Fano resonance is in good agreement with the dc conductivity model. Fano resonance is excited due to the interference between a broad continuum and a discrete mode that gives rise to a high-Q asymmetric line shape resonance.[25-28] One of the

remarkable properties of the Fano resonance is the strong confinement of the subradiant electromagnetic energy in the asymmetric resonator which gradually becomes radiative as the structural asymmetry of the resonator increases. Larger asymmetry lowers the *Q* factor of the Fano resonance. However, when the radiative loss is minute for the low asymmetry structure, it becomes comparable to the non-radiative losses (Ohmic loss) which eventually leads to significantly different behaviour of the Fano resonance for PEC, Drude metal, and the dc conductivity of metals.

Discussion:

In this work, we study the strong influence of metallic conductivity on the Fano resonances in planar metasurfaces with different structural asymmetry resonators at the terahertz frequencies. For each metamaterial design, we carried out numerical simulations with metals governed by different conductivity models i.e. PEC (PEC-TASR), dc conductivity (DC-TASR) and Drude conductivity (Drude-TASR) using the frequency domain solver of commercially available CST microwave studio. **Figure 1** shows the schematic diagram and a microscopic image of an array of asymmetric Fano metasurface. The electromagnetic field impinges at normal incidence on the TASR metamaterial array consisting of aluminium (Al) metal arms of thickness 200 nm deposited on 500 μm thick silicon substrate. For the experiment we choose aluminum metal, because for its high terahertz conductivity and the stability of the samples. Asymmetry is introduced in a perfectly symmetric two split gap (situated at the center of the top and bottom arm) resonator by displacing the lower arm split gap by distance '*d*' from the vertical symmetry axis as shown in the Figure 1(a). The distance *d* has been varied from 0.3 μm to 10 μm. We also define an asymmetry parameter ——

, where l_1 and l_2 are the lengths of the two metallic wires that form the TASR. The Fano resonance is excited by the incoming light field (E_y) polarized perpendicular to the TASR gap. Such a resonance excitation is known as trapped mode resonance[26] as its excitation is

forbidden by the symmetry of the metamaterial unit cell structure. Structural symmetry breaking leads to the appearance of extremely sharp narrow linewidth asymmetric lineshape Fano resonance. For the numerical simulations of Fano resonances in DC-TASR, the dc conductivity of aluminium is taken as 3.56×10^7 S/m.[29] Frequency dependent conductivity of aluminium in Drude-TASR is calculated by applying the Drude model, in which the plasma frequency $\omega_p/2\pi$ = 3606 THz and the collision frequency $\Gamma/2\pi$ = 19.6 THz, respectively.[29]

Figure 2(a)-(f) shows the simulated transmission spectra of the PEC-TASR with asymmetry d = 0.3, 0.5, 1, 3, 5 and 10 μm, respectively. We also carried out simulations for the lower asymmetries below 0.3 μm. However, for the lower asymmetries below 0.3 μm, the resonant transmission amplitude is very low (< 0.01) and we were unable to resolve the Fano resonance. Thus we restrict our discussion in this paper to the minimum asymmetry of 0.3 μm. These transmission curves are recorded when the E field is perpendicular to the TASR gap of the structure. Since meta-atoms of these TASR arrays are made up of PEC, the loss mechanism in these structures is only radiative in nature. The highest Q factor of the Fano resonance in PEC-TASR is 328 for the structure with d = 0.3 μm asymmetry. Here, it is important to note that the Q factor of the Fano resonance gradually decreases as the asymmetry is increased, which has also been reported in previous works.[21,23] We observed that the linewidth of the resonance broadens, whereas the transmission amplitude at the resonance dip gradually decreases with increasing asymmetry d. Q factors were calculated by fitting the transmitted intensity spectrum using Fano formula given by

———— .[9, 12, 25] Where a_1, a_2 and b are constant real number, ω_0 is the Fano resonance frequency, and γ is the overall damping rate of the resonance. The Q factor was then estimated as $Q = \omega_0 / 2\gamma$ .We further discuss the comparison between the Fano resonance profiles for the three different conductivity models. **Figure 3(a)-(c)** shows the Fano resonance

behaviour of the PEC-TASR, Drude-TASR and DC-TASR, respectively at low asymmetry of d = 1 µm. PEC-TASR shows extremely sharp resonance with significant amplitude of transmission peak. However, no resonance was observed in the case of Drude-TASR and DC-TASRs. The Q factor for PEC-TASR at d = 1 µm is about 280. The absence of Fano resonance for the case of Drude and dc conductivities could be understood in terms of conductivity behavior, where the excitation of the resonance mode itself requires a critical minimum conductivity at a specific asymmetry. Lower asymmetry structure requires a higher conductivity value in order to give rise to the Fano interference phenomena. At lower structural asymmetries, the radiative and non-radiative losses are comparable and hence even a small difference in the conductivity results in a large change in the surface currents of the two unequal arms of the TASR's, which results in different Q factors and amplitude depth of the Fano resonance in different cases of conductivity models at varying asymmetries. Similarly, figure 3(e)-(g) shows the Fano resonance behaviour of the PEC-TASR, Drude-TASR and DC-TASR for d = 3 µm. Here, it is important to note that the change in transmission amplitude at resonance is largest for PEC-TASR and the lowest for DC-TASR. The Q factors (Q = 46) are equal for dc and Drude conductivities, whereas for PEC case, it is more than five times (Q = 245) greater than other two cases. Fig. 3(i)-(j) displays the transmission spectra for the structures with asymmetry d = 5 µm, where the Q factor for the PEC case is Q = 131, for Drude case Q = 29, and for DC case Q = 26. We note that the Q factor values for the DC and Drude cases are nearly the same.

Based on the simulated design, we carried out the experimental measurements with identical structures that were fabricated using conventional photolithography on 0.5 mm thick double side polished high resistivity (4 kΩ-cm) n type silicon wafers. 200 nm thick aluminium was deposited using thermal evaporation technique. A 10 mm thick silicon substrate with the same properties was attached at the back side of the sample to enable long scan upto 200 ps by

eliminating the Fabry-Perot reflections from the rear face of the substrate. The transmission amplitude is obtained by estimating $|t(\omega)| = |E_S(\omega) \blacksquare E_R(\omega)|$,where $E_S(\omega)$ and $E_R(\omega)$ are Fourier transform of transmitted electric field of the sample and reference pulses, respectively. Figure 3(d), (h) and (l) represent experimental transmission spectra, which have a good agreement with the DC-TASR spectra. Experimental Fano resonance appears at higher frequency in comparison to the simulated spectra, which may be due to small difference between the simulated and the fabricated structures.

Coupling mechanisms between the resonators can be modeled using the equivalent circuit modelling,[30-31] Langrangian formalism,[32-33] coupled mode theory[34] or by using the coupled oscillator model.[35-36] In this work, we theoretically model the observed Fano resonance using the coupled oscillator model, where the 'bright mode' that couples to the incident electromagnetic field interferes with the 'dark mode' that is decoupled from the incident radiation. The two-oscillator model is governed by the following coupled equations,

———

where, x_b and x_d represents the displacement amplitude for bright and dark mode respectively. Q and M are the charge and mass associated to the bright mode and E_0 is the electric amplitude of the incoming EM wave. Solving for x_b and x_d, we can arrive at the susceptibility expression given by,

———————————————————

The real and imaginary part of the susceptibility respectively defines the dispersion and dissipation of the system. The parameters $\omega_{b,d}$ and $\gamma_{b,d}$ are the resonance frequencies and the linewidths of the bright and dark modes, respectively. K is the proportionality factor that

depends on the Q and M. Ω is the coupling constant that depends on the asymmetry parameter (α) and the separation between the individual modes. For the values of K = 3.6×10^{24}, $\omega_d = \omega_T$, and $\omega_b = 3.8 \times 10^{12}$ rad/sec, the Fano curves obtained for PEC-TASR ($\Omega = 0.45 \times 10^{12}$ rad/sec, $\gamma_d = 1 \times 10^8$ rad/sec), DC-TASR ($\Omega = 0.57 \times 10^{12}$ rad/sec, $\gamma_d = 3 \times 10^{10}$ rad/sec) and Drude-TASR ($\Omega = 0.52 \times 10^{12}$ rad/sec, $\gamma_d = 8 \times 10^9$ rad/sec) are shown in inset of Figure 4(a) for asymmetry d = 3 μm, which shows a good agreement with the numerically simulated results. We observe that the damping parameters ($\gamma_{b,d}$) inversely depend on the conductivity and does not change with the asymmetry parameter (α). Whereas, the coupling constant (Ω) depends inversely on the conductivity value and directly on the asymmetry parameter (α). From the analytical curves (inset Figure 4(a)), we see that *Q* factor and the amplitude of the Fano-resonance shows a direct dependence on the conductivity. For instance, PEC-TASR that has higher conductivity value shows higher *Q* factor and larger amplitude compared with the DC-TASR for the same asymmetry parameter (α).

We further highlight the difference between the PEC behaviour and the Drude-DC behaviours in the low and high structural asymmetry regimes in terms of the Fano resonance linewidth and the depth of the resonant transmission. In **Figure 4(a)** and **(b)**, we show simulated transmission spectra at asymmetry of *d* = 3 μm and *d* = 10 μm, respectively for the PEC-TASR, DC-TASR and Drude-TASR. Change in transmission amplitude at the Fano resonance is the highest for PEC and lowest for DC conductivities. *Q* factors for the DC-TASR and Drude-TASR are the same (*Q* = 46), whereas it is more than 5 times larger (*Q* = 245) for PEC at *d* = 3 μm asymmetry case. At higher asymmetry of *d* = 10 μm, the difference between the linewidth of the resonance as well the amplitude depth is not as drastic as for low asymmetry case as shown in Figure 4(b). The respective *Q* factors for the PEC, Drude and DC-TASRs drop down to *Q* = 29, 10 and 8, respectively. This shows the contrasting behaviour of Fano

resonances in the low and high asymmetry regimes. To further confrim the large difference between PEC and the Drude-DC behaviour, we simulated the electric field in the capacitive gaps at the Fano resonance for all the three different conductivities at d = 3 µm as shown in Figure 4(c),(d) and (e). The strongest electric field concentration in the capacitive gaps of the TASRs is observed for the case of PEC, followed by the Drude and the DC-TASRs. The fields in Drude and DC TASRs are much weaker compared to the PEC-TASRs. Tight field confinement in Fano resonators is extremely important for its multifunctional applications such as ultrasensitive sensors and efficient cavities.

The results presented in Figures 3 and 4 show that the behavior of PEC-TASR's even in the terahertz range is very different from DC and Drude-TASR's, especially at the lower asymmetry. We also investigated the behavior of Fano resonances for different conductivity models at varying asymmetry as shown in **Figure 5** that depicts the response of the TASR's in terms of Q factor and the figure of merit (FoM). Figure 5(a) shows the comparison between the Q factors of PEC, DC, Drude, and experimental TASR's for Al metal. We observe that for the PEC-TASR, the Q factors are extremely high at low asymmetry, whereas the difference reduces drastically with increasing asymmetry in the structure and shows saturation effect at about d = 7 µm. The Q factor values of the DC-TASR and Drude-TASR are comparable and show good agreement with those of the experimental results. Slightly higher Q factors are observed in the measurements at lower asymmetry regime, because the Fano resonance is not very accurately measured due to the limited measurement resolution which could result in a different linewidth of the asymmetric Fano peak at lower asymmetries. Figure 5(b) represents the FoM, which is defined as the product of Q factor and transmission intensity (ΔI) of the resonance peak. At low and moderate asymmetries (between 1 µm to 7 µm) FoM of the PEC-TASR is one order of magnitude higher than the other two cases. FoM values for PEC, DC, and Drude-TASR peaks at structural asymmetry of d = 4 µm, 6 µm and 4 µm, respectively.

The peak FoM values for PEC, DC, and Drude-TASR's are 169.43, 5.80 and 9.10, respectively. Experimental values of FoM for the TASR's are in close agreement with the DC-TASR case. Overall, we observe that at lower asymmetries below 6 μm, conductivity plays a crucial role in determining the Fano resonance linewidth and the transmission amplitude due to low radiative and non-radiative losses. High conductivity materials such as superconductors could excite sharper Fano resonances in comparison to metals at lower asymmetries. However, at higher asymmetries, superconductors and metals would have similar response due to the higher radiative losses.

From the above discussion, it is clear that dc conductivity Al metal and Drude conductivity of metal behaviour is quite similar at higher asymmetries but differs at lower asymmetries of the structure. According to the Drude model for metals, frequency dependent permittivity is given by —— where is the contribution due to the bound carriers. This permittivity in terms of plasma frequency ω_p and damping rate Γ is given by ———. In thin metallic films, where the possible grain boundaries and the crystal defects could contribute to the additional scattering,[37] we can assume that $\omega/\Gamma << 1$ for lower terahertz frequencies. Thus for a conducting metals ( ), permittivity is given by —— The plasma frequency ω_p is given by —— and dc conductivity is given by $\sigma_{dc} = Ne\mu$. Here e is the charge of the electron, m is the effective mass of electron, N is the density of the carriers and μ is the mobility.[37] Here, it is important to note that the conductivity is frequency independent in the terahertz frequency range under the above approximation but permittivity is still a function of frequency. Real part of permittivity is independent of the frequency, whereas the imaginary part shows implicit frequency dependence.

In summary, we have discussed three different scenarios in which we have PEC, Drude conductivity with frequency dependent characteristics and dc conductivity of metal. The dc conductivity case closely matches with experimental results. It is to be noted that dc conductivity case is a special case of Drude conductivity at terahertz frequencies. We found that there is a strong influence of conductivity that plays a vital role in determining the Q factor and the amplitude of the Fano resonances for low structural asymmetry in terahertz asymmetric Fano metasurfaces. Higher conductivity materials are desired to excite sharper resonances at low asymmetry such as superconductors. For larger asymmetry Fano resonators, the radiative loss in the subwavelength resonators become dominant in comparison to the non-radiative (Ohmic) loss. Thus, the Fano resonance in larger asymmetry metamaterial structures does not depend strongly on the conductivity parameter. Thus our results show that the conductivity becomes a critical parameter while designing high Q metamaterial resonators at lower asymmetries that benefits in choosing an appropriate material for designing high Q metamaterial based sensors and narrow-band filters at THz frequencies.

Figures:

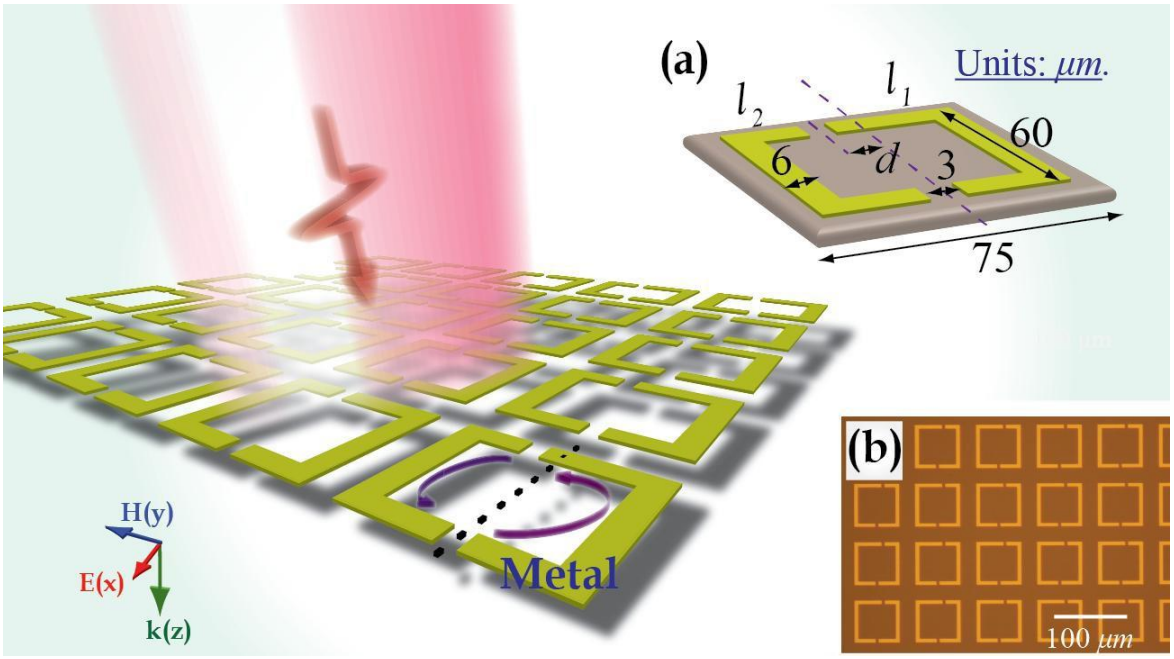

Figure 1: Schematic of the asymmetric metamaterial array: All the dimensions are shown in the unit cell (a) in the figure above. '*d*' is the asymmetry which is the displacement of the lower gap from the central vertical axis. Figure (b) shows optical image of experimentally fabricated sample.

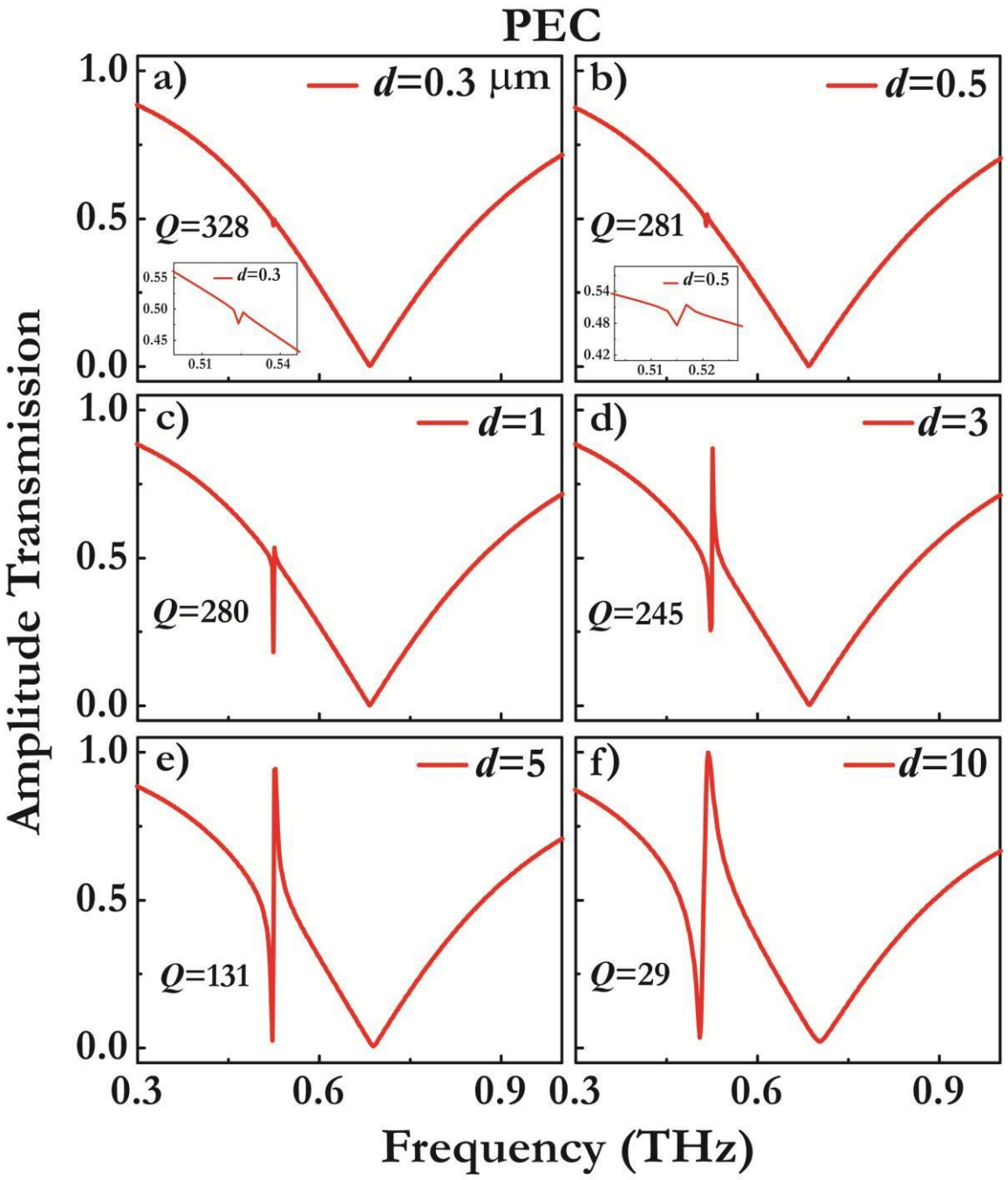

Figure 2:Transmission spectra of PEC Fano metasufaces with varying asymmetry d = 0.3, 0.5, 1, 3, 5 and 10 μm, respectively. Incident electric field is polarized perpendicular to the split gaps.

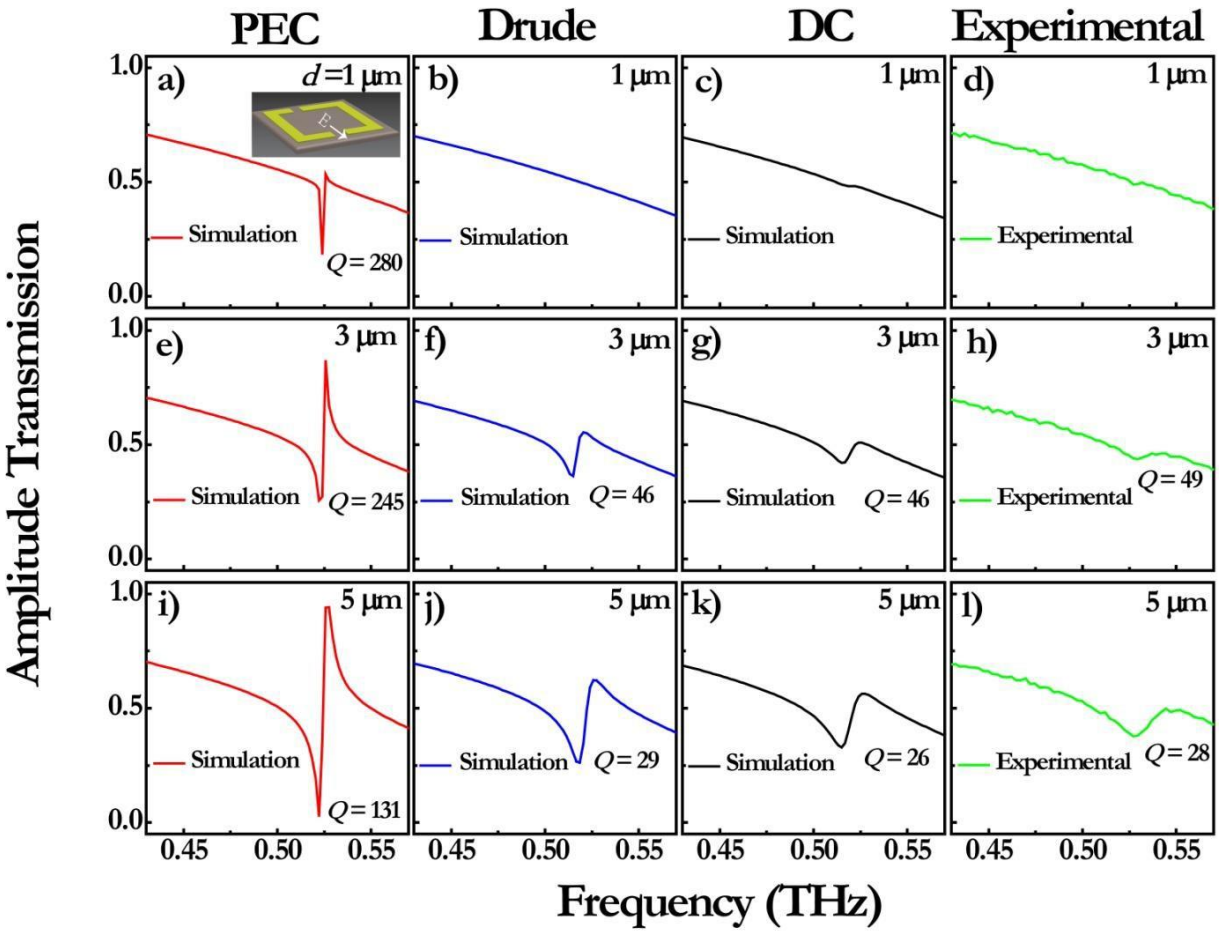

Figure 3: Transmission spectra comparing PEC, Drude, DC, and experimental terahertz asymmetric split-ring resonators: Figure 3(a)-(d) are for TASR's with d = 1 μm, (e)-(h) for d = 3 μm and (i)-(l) for asymmetry d = 5 μm. Figure 3 (d), (h) and (l) represent the measured transmission spectra. Metal in TASR's is assumed to be PEC for Figure 3(a), (e) and (i), Drude metal in (b), (f) and (j) and dc conductivity in (c), (g) and (k).

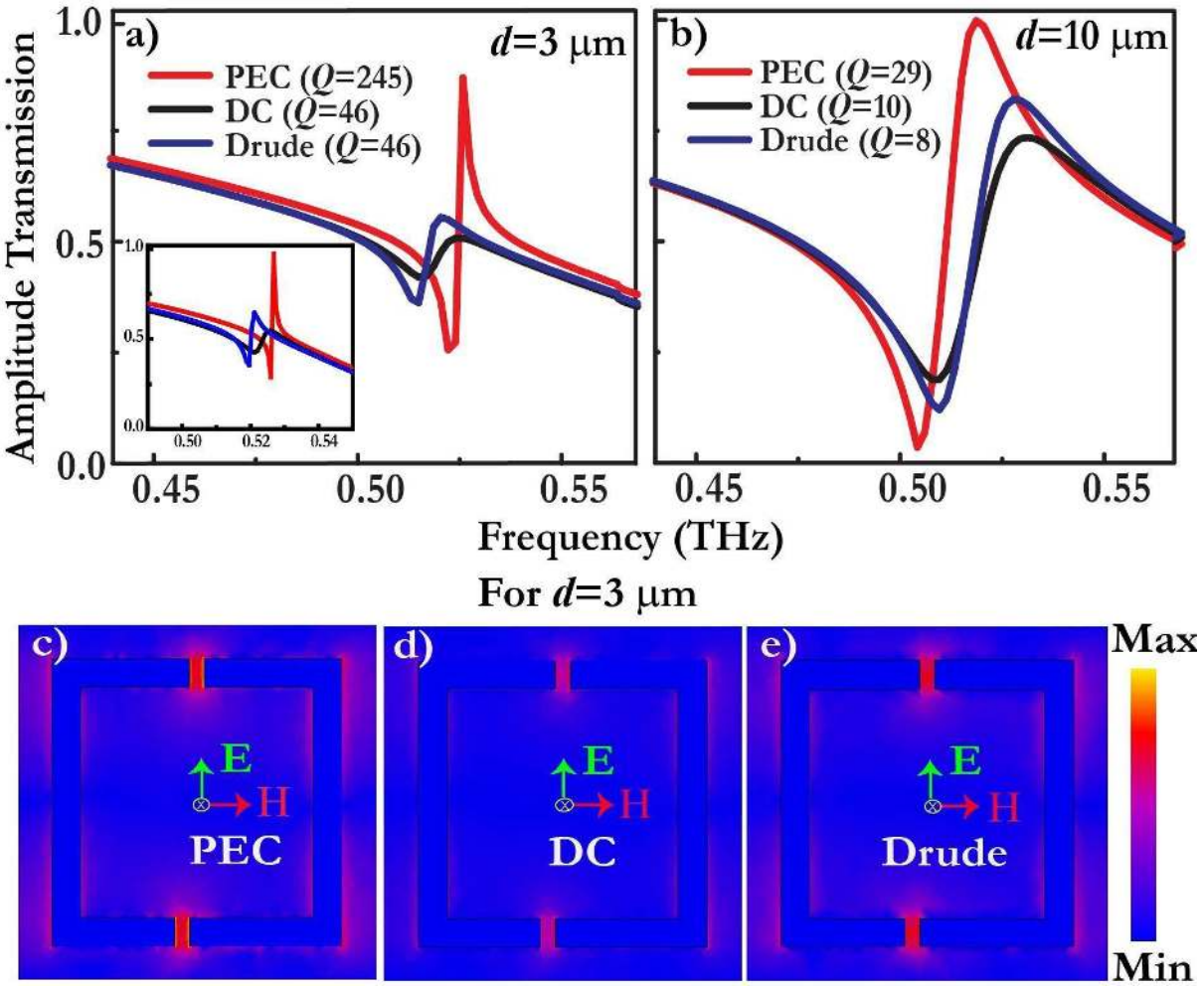

Figure 4: Fano resonance comparison at low and high asymmetry structures: (a) and (b) represent the simulated transmission spectra for PEC-TASR (red), DC-TASR (black) and Drude-TASR (blue) for asymmetry d = 3 and d = 10 μm, respectively. Figure (c)-(e) depicts the simulated electric field distribution at Fano resonance frequency for PEC, DC, and Drude-TASR respectively at asymmetry of d = 3 μm. Inset in Figure (a) represents analytical fit for the Fano resonances using the coupled oscillator model.

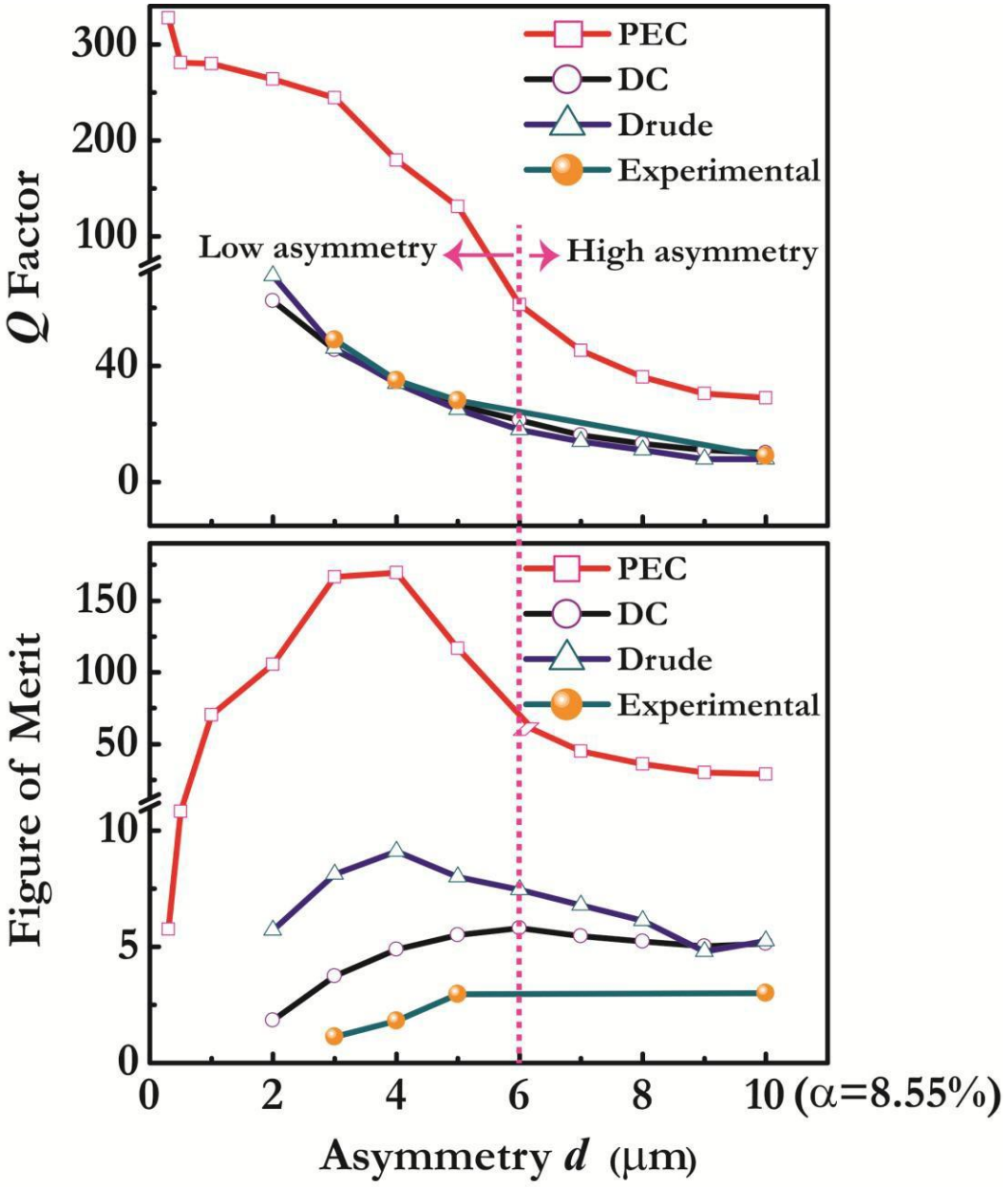

Figure 5: *Q* Factor and FoM comparison for different conductivity models and measurement at varying asymmetry: Graph (a) and (b)display the variation of *Q* factors and FOM respectively, obtained from simulation and experiment with increasing asymmetry *d*in the structure when electric field is applied perpendicular to the gap of the TASR's. Colours in curves represent different conductivity models in TASR's such as PEC (red), DC Al (black), Drude Al (blue) and experimental (cyan).

Refrences:

[1] V. G. Veselago, *Soviet Physics Uspekhi,* **1968**, *10*, 509.

[2] J. B. Pendry, A. J. Holden, D. J. Robbins, W. J. Stewart, *IEEE Trans. Microwave Theory Tech.* **1999**, *47*, 2075.

[3] D. R. Smith, W. J. Padilla, D. C. Vier, S. C.Nemat-Nasser, S. Schultz, *Phys. Rev. Lett.* **2000**, *84*, 4184.

[4] R. A. Shelby, D. R. Smith, S. Schultz, *Science,* **2001**, *292*, 77.

[5] T. J. Yen, W. J. Padilla, N. Fang, D. C. Vier, D. R. Smith, J. B. Pendry, D. N. Basov, X. Zhang, *Science,* **2004**, *303*, 1494.

[6] S. Zhang, D.A. Genov, Y. Wang, M. Liu, X. Zhang, *Phys. Rev. Lett.* **2008,** 101 (4), 047401.

[7] D. Rodrigo, O. Limaj, D. Janner, D. Etezadi, F. J. García de Abajo, V. Pruneri, H. Altug, *Science,* **2015**, *349*, 165.

[8] C. Wu, A. B. Khanikaev, R. Adato, N. Arju, A. A. Yanik, H. Altug, G. Shvets, *Nat. Mater.* **2012**, *11*, 69.

[9] C. Wu, N. Arju, G. Kelp, J. A. Fan, J. Dominguez, E. Gonzales, E. Tutuc, I. Brener, G. Shvets, *Nat. Commun.* **2014**, *5*.

[10] R. Singh, W. Cao, I. Al-Naib, L. Cong, W. Withayachumnankul, W. Zhang, *Appl. Phys. Lett.* **2014**, *105*, 171101.

[11] N. I. Zheludev, S. L. Prosvirnin, N. Papasimakis, V. A. Fedotov, *Nat. Photon.* **2008**, *2*, 351.

[12] Y. Yang, I. I. Kravchenko, D. P. Briggs, J. Valentine, *Nat. Commun.* **2014**, *5*.

[13] A. Boltasseva, H. A. Atwater, *Science,* **2011**, *331*, 290.

[14] S. Xiao, V. P. Drachev, A. V. Kildishev, X. Ni, U. K. Chettiar, H. K. Yuan, V. M. Shalaev, *Nature,* **2010**, *466*, 735.

[15] G. Scalari, C. Maissen, S. Cibella, R. Leoni, J. Faist, *Appl. Phys. Lett.* **2014**, *105*, 261104.

[16] R. Singh, A. K. Azad, J. F. O'Hara, A. J. Taylor, W. Zhang, *Opt. Lett.* **2008**, *33*, 1506.

[17] N. Laman, D. Grischkowsky, *Appl. Phys. Lett.* **2008**, *93*, 051105.

[18] U. Fano, *Phys. Rev.* **1961**, *124*, 1866.

[19] A. E. Miroshnichenko, S. Flach, Y. S. Kivshar, *Rev. Mod. Phys.* **2010**, *82*, 2257.

[20] F. Hao, Y. Sonnefraud, P. V. Dorpe, S. A. Maier, N. J. Halas, P. Nordlander, *Nano Lett.* **2008**, *8*, 3983.

[21] R. Singh, I. A. I. Al-Naib, M. Koch, W. Zhang, *Opt. Express,* **2011**, *19*, 6312.

[22] W. Cao, R. Singh, I. A. I. Al-Naib, M. He, A. J. Taylor, W. Zhang, *Opt. Lett.* **2012**, *37*, 3366.

[23] F. Miyamaru, S. Kubota, T. Nakanishi, S. Kawashima, N. Sato, M. Kitano, and M. W. Takeda, *Appl. Phys. Lett.* **2012**, 101(5), 051112.

[24] K. Aydin, I.M. Pryce, H.A. Atwater, *Opt. Express*, **2010**, 18 (13), 13407.

[25] B. Luk'yanchuk, N. I. Zheludev, S. A. Maier, N. J. Halas, P. Nordlander, H. Giessen, C. T. Chong, *Nat. Mater.* **2010**, *9*, 707.

[26] V. A. Fedotov, M. Rose, S. L. Prosvirnin, N. Papasimakis, N. I. Zheludev, *Phys. Rev. Lett.* **2007**, *99*, 147401.

[27] N. Dabidian, I. Kholmanov, A. B. Khanikaev, K. Tatar, S. Trendafilov, S. H. Mousavi, C. Magnuson, R. S. Ruoff, G. Shvets, *ACS Photonics,* **2015**, *2*, 216.

[28] S. H. Mousavi, I. Kholmanov, K. B. Alici, D. Purtseladze, N. Arju, K. Tatar, D. Y. Fozdar, J. W. Suk, Y. Hao, A. B. Khanikaev, R. S. Ruoff, G. Shvets, *Nano Lett.* **2013**, *13*, 1111.

[29] M. A. Ordal, L. L. Long, R. J. Bell, S. E. Bell, R. R. Bell, R. W. Alexander, C. A. Ward, *Appl. Opt.* **1983**, *22*, 1099.

[30] N. Papasimakis, V. A. Fedotov, and N. I. Zheludev, *Phy. Rev. Lett.* **2008**, *101*, 253903.

[31] E. Tatartschuk, N. Gneiding, F. Hesmer, A. Radkovskaya, and E. Shamonina, *J. Appl. Phys.* **2012***,111*, 094904**.**

[32] D. A. Powell, M. Lapine, M. V. Gorkunov, I. V. Shadrivov, and Y. S. Kivshar, *Phy. Rev. B.* **2010***, 82*, 155128.

[33] M. Liu, D. A. Powell, I. V. Shadrivov, and Y. S. Kivshar, *Appl. Phys. Lett.* **2012***,100*, 111114, **.**

[34] M. Liu, D. A. Powell, I. V. Shadrivov, M. Lapine and Y. S. Kivshar, *New J. Phys.* **2013***,15*, 073036**.**

[35] C.C. L. Garrido Alzar, M. A. G. Martinez, and P. Nussenzveig, *Am. J. Phys*. **2002,***70*, 37.

[36] F.Y. Meng, Q. Wu, D. Erni, K. Wu, and J.C. Lee, *IEEE Trans. Microwave Theory Tech*. **2012**, *60*, 3013.

[37] Y. Zhao, D. Grischkowsky, *IEEE Trans. Microwave Theory Tech.* **2007**, *55*, 656.